



## Article

# Kinetic Modeling of an Enzyme Membrane Reactor for the Selective Production of Oligosaccharides

Shusaku Asano <sup>1,\*</sup> , Yosuke Muranaka <sup>2</sup>, Taisuke Maki <sup>2</sup>, Koki Ikeda <sup>2</sup> and Kazuhiro Mae <sup>2</sup><sup>1</sup> Institute for Materials Chemistry and Engineering, Kyushu University, Kasuga 816-8580, Japan<sup>2</sup> Department of Chemical Engineering, Graduate School of Engineering, Kyoto University, Kyoto 615-8510, Japan

\* Correspondence: shusaku\_asano@cm.kyushu-u.ac.jp

**Abstract:** An enzyme membrane reactor is an attractive tool for producing oligosaccharides from biomass-based polysaccharides. However, kinetic modeling and reactor design based on the rate equations have rarely been reported for enzyme membrane reactors because of the difficulty in tracing the depolymerization process. In this study, a simplified reaction model based on Michaelis–Menten-type kinetics has been built to simulate the enzyme membrane reactor. Ramping various species into reactant, target, and byproduct worked well for discussing reactor performance. The use of a membrane with a molecular weight cut-off (MWCO) of 10 kDa with continuous feeding of the reactant was suggested for the efficient production of chitosan hexamer and pentamer by enzymatic hydrolysis of chitosan.

**Keywords:** enzyme membrane reactor; kinetic modeling; MWCO; chitosan oligosaccharides



**Citation:** Asano, S.; Muranaka, Y.; Maki, T.; Ikeda, K.; Mae, K. Kinetic Modeling of an Enzyme Membrane Reactor for the Selective Production of Oligosaccharides. *Fermentation* **2022**, *8*, 701. <https://doi.org/10.3390/fermentation8120701>

Academic Editors: Yaohua Zhong and Yinbo Qu

Received: 11 November 2022

Accepted: 30 November 2022

Published: 2 December 2022

**Publisher's Note:** MDPI stays neutral with regard to jurisdictional claims in published maps and institutional affiliations.



**Copyright:** © 2022 by the authors. Licensee MDPI, Basel, Switzerland. This article is an open access article distributed under the terms and conditions of the Creative Commons Attribution (CC BY) license (<https://creativecommons.org/licenses/by/4.0/>).

## 1. Introduction

An enzyme membrane reactor uses an ultrafiltration membrane with an enzyme. An ultrafiltration membrane has two synergetic benefits for oligosaccharides production by enzymes. First, the membrane enables the separation of the product and enzyme. Second, the molecular weight distribution of the product can be controlled by the membrane, which rejects undesirable larger molecules to permeate. Thus, enzyme membrane reactors have been intensively studied for the production of oligosaccharides [1]. Target products are usually biomass-based oligomers, such as cello-oligosaccharides [2], galactooligosaccharides [3,4], chitosan oligosaccharides [5], oligodextrans [6], fructooligosaccharides [7,8], and pectin [9]. These oligosaccharides have various applications in the food and feed industry [10–12].

Previous studies on the enzyme membrane reactor often featured optimizing enzyme properties or operating parameters. For example, Qin et al. investigated the gene cloning and expression of a novel chitosanase from *Bacillus amyloliquefaciens* to produce chitosan oligosaccharides in a membrane reactor [13]. Su et al. immobilized dextranase on a polyethersulfone membrane surface and discussed its effect on molecular weight distribution of the product [6]. The influence of the operating conditions, such as flow rate, reactant concentration, enzyme loading, pH, and temperature, have been intensively studied for each reaction system [3,5,9].

Regarding scale-up for industrial production, modeling and simulation of the reaction system are very important [14–16]. However, such modeling study is rarely reported for enzyme membrane reactors [17,18]. One possible reason is the difficulty in simulating the depolymerization of biomass-based polysaccharides. They show a wide variety in molecular weight, chain branching, composition variations, and different crystallinity. Even if a strict characterization of a particular feedstock and mechanistic analysis of its hydrolysis process were achieved, such a fine-tuned model lacks generality and practicality for industrial usage.

In this study, we have built a kinetic model for chitosan oligosaccharide production with a simplified reaction scheme. The reaction model was built as simply as possible, focusing on the reaction profile regarding the target oligomers of hexamer and pentamers. Chitosan hexamer and pentamer production using enzyme membrane reactors have been intensively studied [5,13,19] because these oligomers have attractive antibacterial activities, antitumor activities, and immunoenhancing effects. Based on the reaction and permeation model, we achieved quantitative performance comparison of enzyme membrane reactors.

## 2. Methodology

### 2.1. Materials

Chitosanase, *Streptomyces* sp. N174, was obtained from EMD Millipore Corp (Burlington, MA, USA). The molecular weight of the chitosanase is 95 kDa [19]. Chitosan from *Chionoecetes opilio* (Chitosan 100, over 80 mol% deacetylated) was purchased from Wako Pure Chemical Industries (Tokyo, Japan). Chitosan oligosaccharides were obtained from TCI (Tokyo, Japan). Acetic acid, sodium hydroxide, and sodium acetate were purchased from Wako and used as received. Ultra-purified water was prepared using a Milli-Q water purification system and was used throughout the experiment. Commercial membrane modules (Minimate™ Tangential Flow Filtration Capsule, Pall, MA, USA) with an effective membrane area of 50 cm<sup>2</sup> were used. They contain ultrafiltration membranes made of polyethersulfone with a molecular weight cut-off (MWCO) of 1 k, 3 k, 10 k, or 30 k. Polyethersulfone is exclusively employed for the ultrafiltration of chitosan due to its high fouling resistance and durability [5,20,21].

### 2.2. Batch Hydrolysis

Buffer solution (pH 6.0) was prepared from acetic acid and sodium hydroxide. Chitosan was dissolved in the buffer solution by a vigorous stirring of 8 h. The concentration of chitosan was adjusted to 10 g/L. A total of 5 mL of the chitosan solution was mixed with 0.036 mL of chitosanase solution containing 1 U of the enzyme. Soon after the mixing, the reaction was carried out at 40 °C with stirring by a magnetic stirrer (KPI, Itami, Japan). After a reaction time of 0.5–24 h, the solution was boiled to terminate the enzymatic reaction. The concentrations of chitosan oligosaccharides from dimer to hexamer were measured by high-performance liquid chromatography (HPLC, Shimadzu). A refractive index detector (RID-10A) was employed. A CAPCELL PAK NH<sub>2</sub> SG80 column (Shiseido, Tokyo, Japan) was used at 45 °C. The mobile phase was an acetonitrile/water mixture (75/25 in volume). The flow rate was 1 mL/min. The concentration of each oligosaccharide was calculated from each peak area. Chitosan oligosaccharide reagent was used as the standard. The chitosan sample was diluted with the mobile phase, and precipitated chitosan polymer was filtered out before analysis. One experiment and analysis were performed for each condition in this study, following the relevant studies [3,5,22].

### 2.3. Membrane Permeation

The fundamental permeation property of the membrane against chitosan oligosaccharides and chitosan polymers was evaluated in a filtration process without a chemical reaction (Figure 1). Stock solution of chitosan oligosaccharide (1, 5, or 10 g/L) or chitosan polymer solution after 1 h batch hydrolysis was fed to the ultrafiltration membrane modules. The permeate flow rate was set at 10, 25, or 100 mL/h. The retentate flow rate was adjusted to be the same as the permeate flow rate by using the back pressure regulator. The permeate solution was analyzed by HPLC. The permeation of chitosan polymer was quantified by precipitating out the polymer from the permeate solution with HPLC mobile phase. Rejection rate  $R$  was calculated as follows:

$$R = 1 - \frac{\text{permeate concentration}}{\text{stock solution concentration}}$$

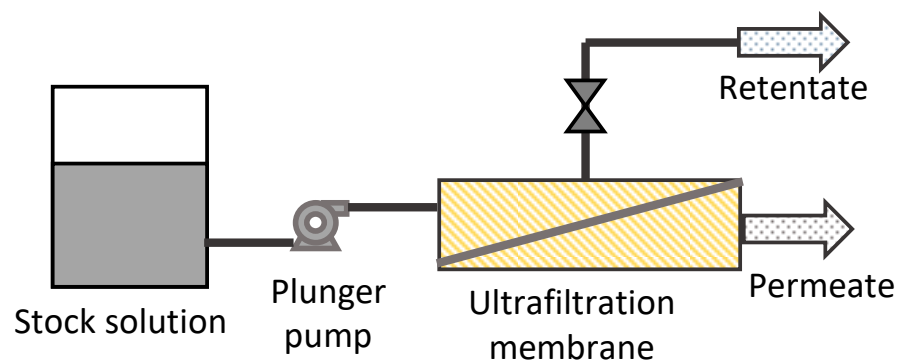


**Figure 1.** Permeation test system.

#### 2.4. Continuous Hydrolysis with Membrane Reactor

An enzyme membrane reactor was composed, as shown in Figure 2. A total of 10 g/L of chitosan solution containing chitosanase with a concentration of 100 U/L was charged in a beaker. The charging volume was 100–600 mL. A plunger pump carried the reacting solution to the membrane module at the flow rate of 600 mL/h. A back pressure regulator adjusted the product stream flow rate at 100 mL/h. The pressure at the pump head was less than the pressure limit of the membrane module of 4 bar in all conditions. The retentate solution was recycled into the reactor. Chitosan 10 g/L solution without chitosanase was continuously fed to the reactor at the flow rate of 100 mL/h to realize the continuous operation. Throughout the operation, the reaction mixture was stirred by a magnetic stirrer, and the reactor temperature was kept at 40 °C. A steady state was typically reached after three times the mean residence time had passed.

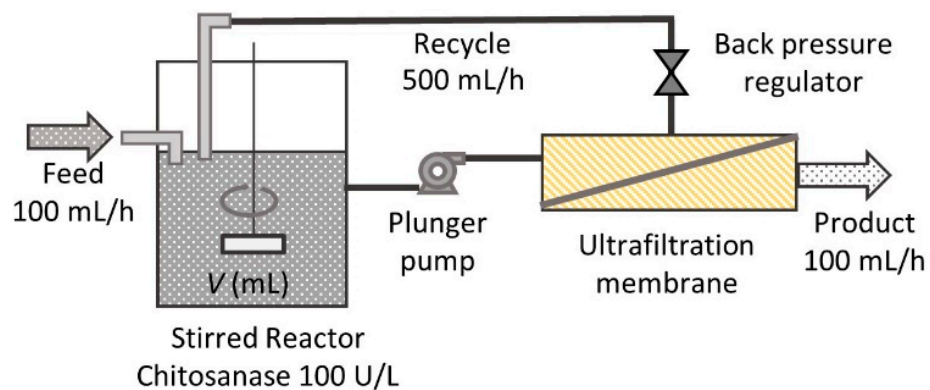


**Figure 2.** Enzyme membrane reactor setup.

### 3. Results and Discussion

#### 3.1. Reaction Modeling and Permeation Evaluation

Figure 3 presents the reaction profile in a batch reactor. *Streptomyces* sp. N174 hydrolyzes chitosan in an endo-splitting manner [23]. It has no ability to produce a monomer. Thus, dimers and trimers are not hydrolyzable by chitosanase. In contrast, the target product of hexamers and pentamers can be further hydrolyzed to dimers, trimers, and tetramers. The concentration of the hexamers and pentamers increased and then decreased after peaking by the overreaction. The concentration of dimer and trimer, the final products of the enzymatic hydrolysis, increased monotonically. The overall tendency agrees well with the previous report [5]. An ultrafiltration membrane is attractive for the selective separation of the intermediate hexamer and pentamer from the reaction mixture containing the chitosanase to avoid further degradation of the target products.

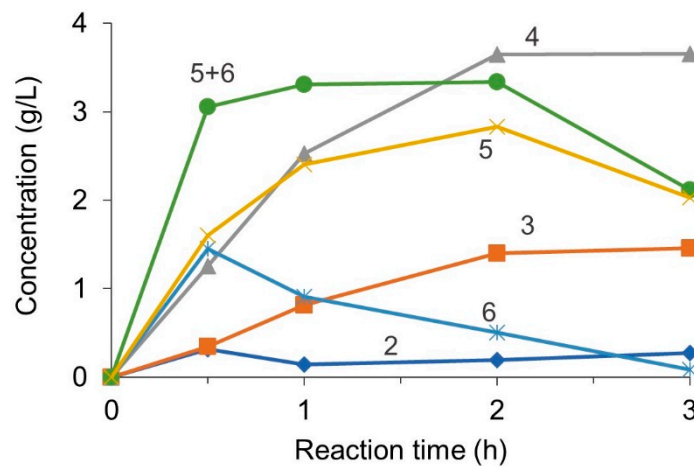


**Figure 3.** Profile of chitosan oligosaccharide concentration in a batch reactor. Numbers indicate the degree of polymerization of the oligosaccharides.

Even after 24 h of reaction, the total concentration of chitosan oligomers was 8.5 g/L, indicating that 15 wt% of the input chitosan was unconvertible to oligomers. The deacetylation ratio of the chitosan reagent was over 80 mol%. Because the chitosanase cannot split GlcNAc-GlcNAc linkages [23], the remaining 15 wt% component can be attributed to the N-acetyl-D-glucosamine units. The yield of each oligosaccharide is, thus, defined as follows:

$$\text{oligomer yield} = \frac{\text{obtained oligomer amount}}{\text{total amount of hydrolyzable unit}} = \frac{\text{obtained oligomer amount}}{\text{input chitosan amount} \times (1 - 0.15)}$$

With the definition above, the sum of the hexamer and pentamer yield was around 39 wt% after 1 h reaction.

We considered a simplified chitosan hydrolysis reaction model shown in Figure 4. Because our focus was the selective production of a specific range of oligomers, the hydrolysis products were ramped into desired oligomers (B) and undesired smaller oligomers (C). Oligomers and polymers larger than desired oligomers were ramped into the reactant (A). A series-parallel type reaction was considered. Additionally, C generation pathways from A and B were considered.

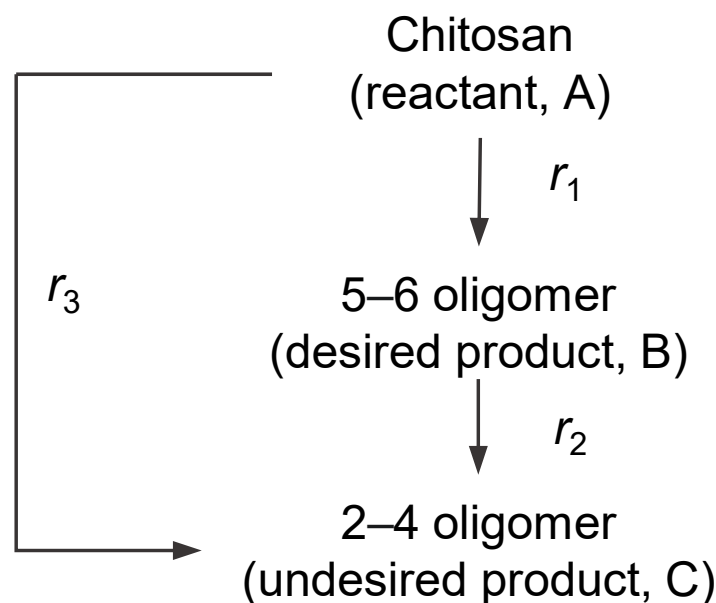


**Figure 4.** Simplified reaction pathways in a series-parallel type reaction scheme.

For the reaction rate expression, the Michaelis–Menten-type equations were used. Because chitosanase can bind not only to digestible chitosan but also to undigestible chitosan trimer and dimer [24], all the reactants and products were included in the denominator.

$$r_1 = \frac{v_{\max,1}[A]}{K_{m1} + ([A] + [B] + [C])}$$

$$r_2 = \frac{v_{\max,2}[B]}{K_{m2} + ([A] + [B] + [C])}$$

$$r_3 = \frac{v_{\max,3}[A]}{K_{m3} + ([A] + [B] + [C])}$$

Boucher et al. reported the Michaelis constant  $K_m$  of the chitosanase *Streptomyces* sp. N174 for chitosan hydrolysis as 0.0293 g/L [25]. This value is employed for  $K_{m1}$ ,  $K_{m2}$ , and  $K_{m3}$  in this study. Although the actual values of the above Michaelis constants would differ for each reaction, the reactant concentration in this study is 10 g/L. Industrial applications would also employ the same range or even higher reactant concentrations. Thus, errors in the Michaelis constants are unimportant for the kinetic modelling of our interests. Values of  $v_{\max,1}$ ,  $v_{\max,2}$ , and  $v_{\max,3}$  were obtained (Table 1), by parameter fitting with the Levenberg–Marquardt method. For the parameter fitting, the following ordinary differential equations were solved with the backward differentiation formula:

$$\frac{d[A]}{dt} = -r_1 - r_3$$

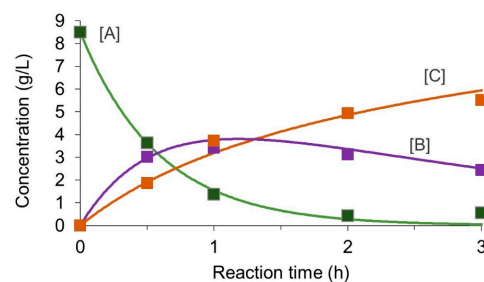
$$\frac{d[B]}{dt} = r_1 - r_2$$

$$\frac{d[C]}{dt} = r_2 + r_3$$

**Table 1.** Kinetic parameters for the enzymatic hydrolysis of chitosan.

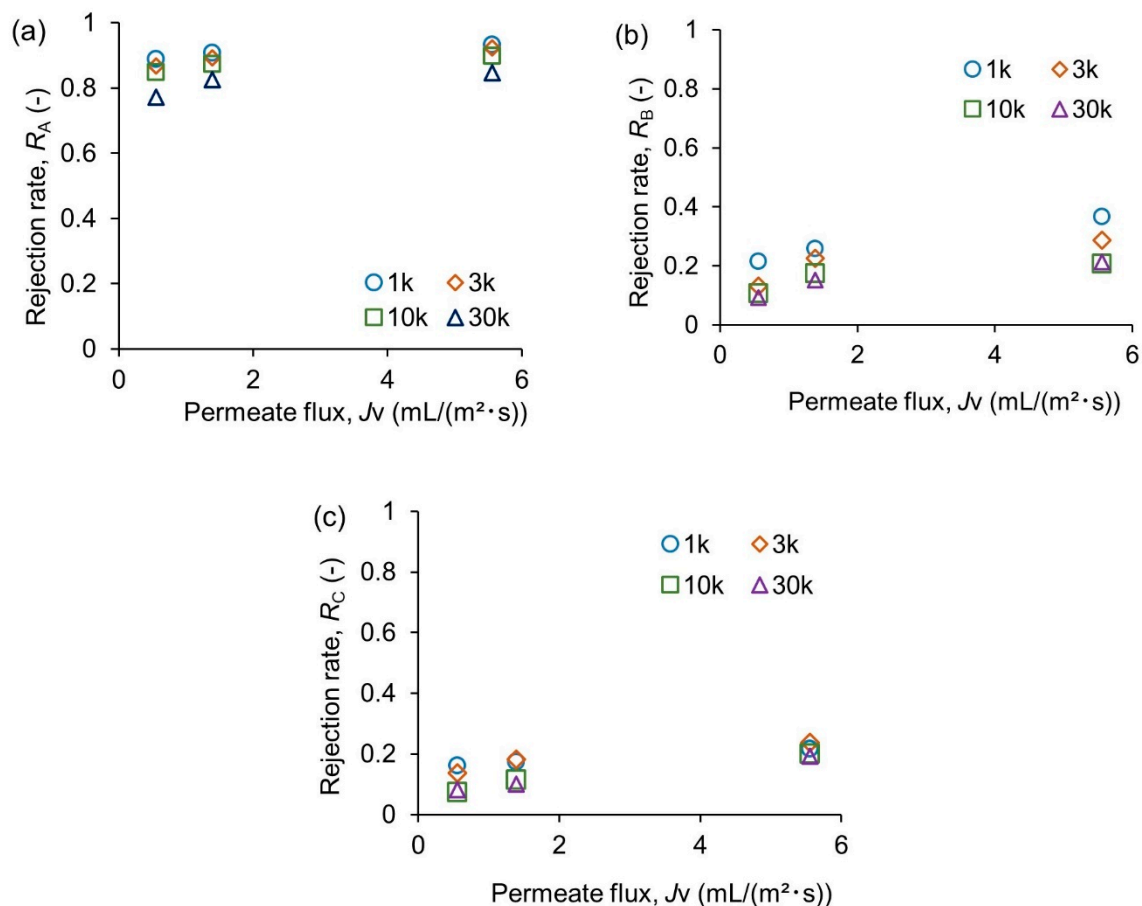
	Value (h <sup>-1</sup> )	Standard Error		Correlation Coefficient		
		(h <sup>-1</sup> )	(%)	$v_{\max,1}$	$v_{\max,2}$	$v_{\max,3}$
$v_{\max,1}$	9.64	0.502	5.2	1	-	-
$v_{\max,2}$	2.91	0.273	9.4	0.49	1	-
$v_{\max,3}$	4.78	0.436	9.1	-0.318	-0.797	1

Figure 5 shows the fitted curves with the experimental results. Note that [A] was based on the D-glucosamine unit (85 wt% of the initial amount). The fitting curve matched well with the experimental results.



**Figure 5.** Model fitting to the reaction profile in a batch reactor. Markers indicate the experimental values. Lines indicate the simulated value. [A], [B], and [C] is a concentration of reactant, desired product, and undesired product, respectively.

Next, the permeation performance of the membrane was evaluated. Figure 6 summarizes the results. In all cases, increased permeate flux resulted in higher rejection due to the concentration polarization effect [26]. The hexamer and pentamer have molecular weights of 823.8 and 985.0, respectively. A MWCO of 1k is the best for rejecting the permeation of the polymers larger than the target range based on the molecular weight. However, the rejection of chitosan was 89–93% with 1k MWCO (Figure 6a). These values differed only 1% from those with 3 k MWCO. Slight permeation of molecules with much higher molecular weights than MWCO was commonly reported [27,28]. The membrane pore size distribution or dynamic behavior of polymer molecules might be responsible for the permeation. In contrast, the permeation of the target oligomers was significantly affected by MWCO (Figure 6b). Rejection of target oligomers with 1 k MWCO reached 36% at the highest permeate flux of 5.6 mL/(m<sup>2</sup>·s). A MWCO of 10k achieved a 15% smaller rejection at the same flux than a MWCO of 1 k. Enlargement of MWCO to 30 k did not further improve the permeability. Permeation resistance would shift from the membrane's pore to the boundary layer in the solution [29]. According to these results, it is expected that neither 1k MWCO nor 30 k MWCO is suitable for a membrane reactor. High resistance to the product permeation or leaching of a large polymer will cause troubles with these membranes. Since enzyme activity can be affected by pressure applied for the membrane permeation [17], using a 10 k membrane might be the best choice to retain the reactant and separate the products.



**Figure 6.** Permeation characteristics of membranes. (a) Chitosan polymer after 1 h hydrolysis, (b) target oligosaccharides (hexamer and pentamer), and (c) undesirable smaller oligosaccharides (dimer, trimer, and tetramer).

### 3.2. Reactor Modeling and Comparison

Based on the established reaction model and permeation performance, we have simulated reactors with different operation modes and membrane MWCOs. Figure 7 illustrates the operation modes. A membrane reactor can be operated in a semi-batch mode [13,18] (Figure 7b) or a continuous mode [3,5] (Figure 7c). In the semi-batch mode, the product solution flows out continuously. Buffer solution without reactant flows in at the same flow rate as the product so that the reaction volume is constant. The operation continues until only a small amount of reactants and products are in the reactor. In the continuous mode, the reactant solution without enzyme flows in. If the membrane performance and the enzyme activity are constant, the reactor can be in a steady state. Mean residence time (reactor volume/reactant flow rate) is crucial for continuous operation.

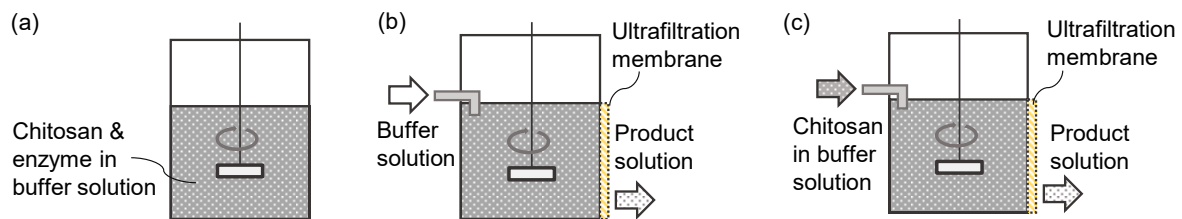


**Figure 7.** Reactor operation modes. (a) Batch reactor, (b) membrane reactor of semi-batch mode with feeding buffer solution, (c) membrane reactor of continuous mode with feeding reactant solution.

The mass balance equations for a semi-batch reactor are as follows:

$$\frac{d[A]}{dt}V = -r_1V - r_3V - (1 - R_A)[A]F$$

$$\frac{d[B]}{dt}V = r_1V - r_2V - (1 - R_B)[B]F$$

$$\frac{d[C]}{dt}V = r_2V + r_3V - (1 - R_C)[C]F$$

where  $R_i$  is the rejection rate of species  $i$ ,  $V$  is the reactor volume, and  $F$  is the product flow rate. These equations were solved numerically.

Concentrations of the continuous membrane reactor can be solved analytically from the following mass balance equations:

$$F[A]_{in} = F[A]_{out} + F[B]_{out} + F[C]_{out}$$

$$F[A]_{out} - F[A]_{in} = -r_1V - r_3V$$

$$F[B]_{out} = r_1V - r_2V$$

$$F[C]_{out} = r_2V + r_3V$$

where  $[i]_{in}$  is the concentration of species  $i$  in the feed flow, and  $[i]_{out}$  is the concentration of species  $i$  in the product flow. Furthermore,  $[i]_{out}$  can be calculated from the concentration in the reactor as follows:

$$[i]_{out} = (1 - R_i)[i]$$

Figure 8 presents the simulated yield against the operation time or the mean residence time. The initial concentration and the feeding concentration of chitosan was 1 wt%. The product flow rate was 100 mL/h for semi-batch and continuous operations. In the batch reactor, the B yield reaches the maximum at around 1.2 h and then decreases due to the overreaction. In the simulation of a semi-batch operation, the reactor volume was 100 mL, and the product flow rate was 100 mL/h. The yield was defined from the total amount of the target product recovered from the permeate solution. It increased monotonically

with the operation time and approaches the plateau. In the simulated case, the final yield was 60% at around 12 h of operation. The semi-batch mode improved the yield by 15% compared to the batch reactor. However, productivity per reactor volume per operation time decreased significantly due to the permeation resistance of the product. Increasing the product flow rate would help to shorten the operation time but would result in a diluted product solution. The continuous mode achieved a higher yield than the batch reactor with enhanced productivity. A larger MWCO value resulted in a lower yield due to reactant loss. In the case of an ideal membrane with 100% rejection of A and 0% rejection of B and C, yield and productivity can be further improved, as shown in the red line in Figure 8. Continuous feeding of the chitosan and recycling of the retentate results in the accumulation of the chitosan in the reactor. If the residence time is too short, it ends up with the chitosan concentration higher than the solubility limit of 5 wt%. The left ends of the curves in the Figure 8 indicate that the chitosan concentration in the reactor reaches 5 wt% at the steady state.

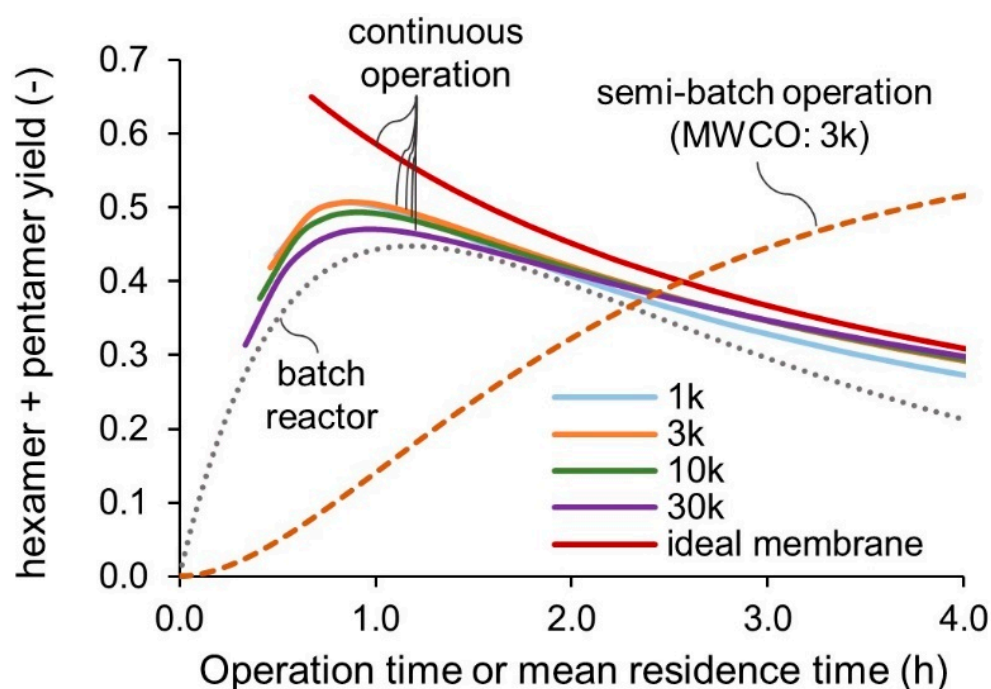


**Figure 8.** Simulated yield for various reactors and membrane performances. The left ends of the curves indicate that the chitosan concentration in the reactor reaches 5 wt%.

### 3.3. Experimental Validation

According to the simulations, continuous operation with a membrane of 3 k or 10 k MWCO would be desirable. Continuous operation of the membrane reactor was conducted, as shown in Figure 2. The mean residence time was adjusted by changing the reactor volume from 100 mL to 600 mL while keeping the feed flow rate. The results are shown in Figure 9. As in the model calculation, MWCOs of 3 k and 10 k resulted in a similar yield. Previous studies on chitosan oligosaccharide production with enzyme membrane reactors employed MWCOs of 2–5 k [5,13,19]. No significant difference in the selectivity by MWCO is expected in these ranges. However, regarding scale-up for industrial production, a larger MWCO of 10 k might be better for pressure reduction and fouling prevention.

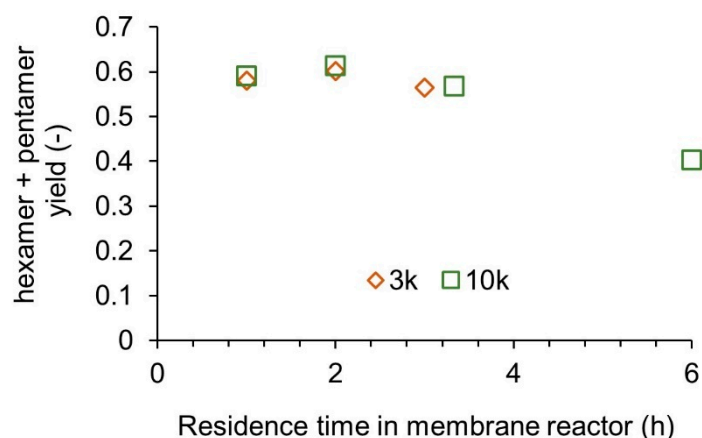


**Figure 9.** Experimental results for continuous membrane reactors with feeding reactant solution.

Although the overall tendency against the residence time was similar, the maximum yield and optimum residence time differed vastly from the model prediction—a 10% higher yield than the model prediction was obtained. The rejection rate of chitosan was obtained using the semi-hydrolyzed solution for 1 h in the batch reactor. The actual rejection of the chitosan would be much higher at the initial stage of the hydrolysis. The longer residence time for the maximum yield might be attributed to the binding inhibition by chitin components. Although GlcNAc-GlcNAc bonding cannot be hydrolyzed, it can interact with chitosanases [24].

#### 4. Conclusions

Simplified reaction rate equations and membrane permeation performances were combined to simulate membrane reactors. The optimal operation mode and MWCO value for selective and efficient production of chitosan oligosaccharides were discussed based on the simulation and validated experimentally. The following conclusions were drawn:

- (1) A tight membrane with a small MWCO value close to the target oligomer does not necessarily improve the reactor performance. Complete rejection of larger oligomers is difficult, even with the smallest MWCO. A coarse membrane with a larger MWCO is recommended to reduce the fouling risks and operating pressure;
- (2) Rejection of the membrane permeation concentrates the reacting medium at the residue side. Thus, a membrane reactor with continuous feeding of the reactant and recycling of the retentate solution can produce a higher yield in a shorter residence time than the batch reactor;
- (3) A membrane reactor with the semi-batch operation mode can obtain the target oligomer in a higher yield than with the continuous operation mode. However, the productivity is lower than the batch reactor because the permeation rate and concentration of the product are in a trade-off relationship;
- (4) Experimental results have an acceptable agreement with the model prediction. The membrane reactor model with the simplified reaction rate equations helps in designing the reactor blueprint. The discrepancy in the optimum residence time and yield will be reduced by considering the binding inhibition effect.

We employed commercial polyethersulfone membranes in this study. Considering the difficulty of completely rejecting large molecular weight components (Figure 6a), the development of novel polyethersulfone-based membranes [30–32] is essential for future studies further to increase the performance of the enzyme membrane reactors.

**Author Contributions:** Conceptualization, T.M. and S.A.; methodology, Y.M. and T.M.; validation, S.A.; formal analysis, S.A.; investigation, T.M. and Y.M.; resources, T.M.; data curation, K.L.; writing—original draft preparation, S.A.; writing—review and editing, Y.M. and T.M.; supervision, K.M.; project administration, K.M.; funding acquisition, S.A. All authors have read and agreed to the published version of the manuscript.

**Funding:** This research was funded by JSPS KAKENHI (Grant number JP21H05083).

**Institutional Review Board Statement:** Not applicable.

**Informed Consent Statement:** Not applicable.

**Data Availability Statement:** The data presented in this study are available in this article.

**Acknowledgments:** S.A. acknowledges the support from the Cooperative Research Program of Network Joint Research Center for Materials and Devices that has been supported by the Ministry of Education, Culture, Sports, Science, and Technology (MEXT), Japan. All the authors acknowledge the support from Council for Science, Technology and Innovation (CSTI), Cross-ministerial Strategic Innovation Promotion Program (SIP), “Technologies for Smart Bioindustry and Agriculture” administered by Bio-oriented Technology Research Advancement Institution, and National Agriculture and Food Research Organization.

**Conflicts of Interest:** All the authors declare no conflict of interest.

## References

1. Su, Z.; Luo, J.; Li, X.; Pinelo, M. Enzyme Membrane Reactors for Production of Oligosaccharides: A Review on the Interdependence between Enzyme Reaction and Membrane Separation. *Sep. Purif. Technol.* **2020**, *243*, 116840. [[CrossRef](#)]
2. Karnaouri, A.; Matsakas, L.; Bühler, S.; Muraleedharan, M.N.; Christakopoulos, P.; Rova, U. Tailoring Celluclast® Cocktail’s Performance towards the Production of Prebiotic Cello-Oligosaccharides from Waste Forest Biomass. *Catalysts* **2019**, *9*, 897. [[CrossRef](#)]
3. Das, R.; Sen, D.; Sarkar, A.; Bhattacharyya, S.; Bhattacharjee, C. A Comparative Study on the Production of Galacto-Oligosaccharide from Whey Permeate in Recycle Membrane Reactor and in Enzymatic Batch Reactor. *Ind. Eng. Chem. Res.* **2011**, *50*, 806–816. [[CrossRef](#)]
4. Botelho, V.A.; Mateus, M.; Petrus, J.C.C.; de Pinho, M.N. Membrane Bioreactor for Simultaneous Synthesis and Fractionation of Oligosaccharides. *Membranes* **2022**, *12*, 171. [[CrossRef](#)]
5. Kuroiwa, T.; Izuta, H.; Nabetani, H.; Nakajima, M.; Sato, S.; Mukataka, S.; Ichikawa, S. Selective and Stable Production of Physiologically Active Chitosan Oligosaccharides Using an Enzymatic Membrane Bioreactor. *Process Biochem.* **2009**, *44*, 283–287. [[CrossRef](#)]
6. Su, Z.; Luo, J.; Pinelo, M.; Wan, Y. Directing Filtration to Narrow Molecular Weight Distribution of Oligodextran in an Enzymatic Membrane Reactor. *J. Membr. Sci.* **2018**, *555*, 268–279. [[CrossRef](#)]
7. Ur Rehman, A.; Kovacs, Z.; Quitmann, H.; Ebrahimi, M.; Czermak, P. Enzymatic Production of Fructooligosaccharides from Inexpensive and Abundant Substrates Using a Membrane Reactor System. *Sep. Sci. Technol.* **2016**, *51*, 1537–1545. [[CrossRef](#)]
8. Burghardt; Coletta; van der Bolt; Ebrahimi; Gerlach; Czermak Development and Characterization of an Enzyme Membrane Reactor for Fructo-Oligosaccharide Production. *Membranes* **2019**, *9*, 148. [[CrossRef](#)]
9. Baldassarre, S.; Babbar, N.; Van Roy, S.; Dejonghe, W.; Maesen, M.; Sforza, S.; Elst, K. Continuous Production of Pectic Oligosaccharides from Onion Skins with an Enzyme Membrane Reactor. *Food Chem.* **2018**, *267*, 101–110. [[CrossRef](#)]
10. Moure, A.; Gullón, P.; Domínguez, H.; Parajó, J.C. Advances in the Manufacture, Purification and Applications of Xylo-Oligosaccharides as Food Additives and Nutraceuticals. *Process Biochem.* **2006**, *41*, 1913–1923. [[CrossRef](#)]
11. Swiatkiewicz, S.; Swiatkiewicz, M.; Arczewska-Wlosek, A.; Jozefiak, D. Chitosan and Its Oligosaccharide Derivatives (Chito-Oligosaccharides) as Feed Supplements in Poultry and Swine Nutrition. *J. Anim. Physiol. Anim. Nutr.* **2015**, *99*, 1–12. [[CrossRef](#)] [[PubMed](#)]
12. Nedaei, S.; Noori, A.; Valipour, A.; Khanipour, A.A.; Hoseinifar, S.H. Effects of Dietary Galactooligosaccharide Enriched Commercial Prebiotic on Growth Performance, Innate Immune Response, Stress Resistance, Intestinal Microbiota and Digestive Enzyme Activity in Narrow Clawed Crayfish (*Astacus leptodactylus* Eschscholtz, 1823). *Aquaculture* **2019**, *499*, 80–89. [[CrossRef](#)]
13. Qin, Z.; Luo, S.; Li, Y.; Chen, Q.; Qiu, Y.; Zhao, L.; Jiang, L.; Zhou, J. Biochemical Properties of a Novel Chitosanase from *Bacillus Amyloliquefaciens* and Its Use in Membrane Reactor. *LWT* **2018**, *97*, 9–16. [[CrossRef](#)]
14. Asano, S.; Yatabe, S.; Maki, T.; Mae, K. Numerical and Experimental Quantification of the Performance of Microreactors for Scaling-up Fast Chemical Reactions. *Org. Process Res. Dev.* **2019**, *23*, 807–817. [[CrossRef](#)]
15. Asano, S.; Maki, T.; Nakayama, R.; Utsunomiya, R.; Muranaka, Y.; Kuboyama, T.; Mae, K. Precise Analysis and Control of Polymerization Kinetics Using a Micro Flow Reactor. *Chem. Eng. Process. Process Intensif.* **2017**, *119*, 73–80. [[CrossRef](#)]
16. Asano, S.; Maki, T.; Inoue, S.; Sogo, S.; Furuta, M.; Watanabe, S.; Muranaka, Y.; Kudo, S.; Hayashi, J.; Mae, K. Incorporative Mixing in Microreactors: Influence on Reactions and Importance of Inlet Designation. *Chem. Eng. J.* **2023**, *451*, 138942. [[CrossRef](#)]
17. Fan, R.; Burghardt, J.P.; Dresler, J.; Czermak, P. Process Design for the Production of Prebiotic Oligosaccharides in an Enzyme Membrane Bioreactor: Interaction between Enzymatic Reaction and Membrane Filtration. *Chem. Ing. Tech.* **2021**, *93*, 306–310. [[CrossRef](#)]
18. Al-Mardeai, S.; Elnajjar, E.; Hashaikeh, R.; Kruczek, B.; Al-Zuhair, S. Dynamic Model of Simultaneous Enzymatic Cellulose Hydrolysis and Product Separation in a Membrane Bioreactor. *Biochem. Eng. J.* **2021**, *174*, 108107. [[CrossRef](#)]

19. Sinha, S.; Chand, S.; Tripathi, P. Production, Purification and Characterization of a New Chitosanase Enzyme and Improvement of Chitosan Pentamer and Hexamer Yield in an Enzyme Membrane Reactor. *Biocatal. Biotransform.* **2014**, *32*, 208–213. [[CrossRef](#)]
20. Yildirim-Aksoy, M.; Beck, B.H.; Zhang, D. Examining the Interplay between *Streptococcus agalactiae*, the Biopolymer Chitin and Its Derivative. *MicrobiologyOpen* **2019**, *8*, e00733. [[CrossRef](#)] [[PubMed](#)]
21. Sánchez, Á.; Mengibar, M.; Rivera-Rodríguez, G.; Moerchbacher, B.; Acosta, N.; Heras, A. The Effect of Preparation Processes on the Physicochemical Characteristics and Antibacterial Activity of Chitooligosaccharides. *Carbohydr. Polym.* **2017**, *157*, 251–257. [[CrossRef](#)] [[PubMed](#)]
22. Kuroiwa, T.; Noguchi, Y.; Nakajima, M.; Sato, S.; Mukataka, S.; Ichikawa, S. Production of Chitosan Oligosaccharides Using Chitosanase Immobilized on Amylose-Coated Magnetic Nanoparticles. *Process Biochem.* **2008**, *43*, 62–69. [[CrossRef](#)]
23. Fukamizo, T.; Honda, Y.; Goto, S.; Boucher, I.; Brzezinski, R. Reaction Mechanism of Chitosanase from *Streptomyces* Sp. N174. *Biochem. J.* **1995**, *311*, 377–383. [[CrossRef](#)] [[PubMed](#)]
24. Fukamizo, T.; Yoshikawa, T.; Katsumi, T.; Amano, S.; Miki, K.; Ando, A.; Brzezinski, R. Substrate-Binding Mode of Bacterial Chitosanases. *J. Appl. Glycosci.* **2005**, *52*, 7. [[CrossRef](#)]
25. Boucher, I.; Fukamizo, T.; Honda, Y.; Willick, G.E.; Neugebauer, W.A.; Brzezinski, R. Site-Directed Mutagenesis of Evolutionary Conserved Carboxylic Amino Acids in the Chitosanase from *Streptomyces* Sp. N174 Reveals Two Residues Essential for Catalysis. *J. Biol. Chem.* **1995**, *270*, 6. [[CrossRef](#)]
26. Neggaz, Y.; Vargas, M.L.; Dris, A.O.; Riera, F.; Alvarez, R. A Combination of Serial Resistances and Concentration Polarization Models along the Membrane in Ultrafiltration of Pectin and Albumin Solutions. *Sep. Purif. Technol.* **2007**, *54*, 18–27. [[CrossRef](#)]
27. García, A.; Álvarez, S.; Riera, F.; Álvarez, R.; Coca, J. Sunflower Oil Miscella Degumming with Polyethersulfone Membranes. *J. Food Eng.* **2006**, *74*, 516–522. [[CrossRef](#)]
28. Ren, J.; Li, Z.; Wong, F.-S. A New Method for the Prediction of Pore Size Distribution and MWCO of Ultrafiltration Membranes. *J. Membr. Sci.* **2006**, *279*, 558–569. [[CrossRef](#)]
29. Długołęcki, P.; Ogonowski, P.; Metz, S.J.; Saakes, M.; Nijmeijer, K.; Wessling, M. On the Resistances of Membrane, Diffusion Boundary Layer and Double Layer in Ion Exchange Membrane Transport. *J. Membr. Sci.* **2010**, *349*, 369–379. [[CrossRef](#)]
30. Arahman, N.; Jakfar, J.; Dzulhijjah, W.A.; Halimah, N.; Silmina, S.; Aulia, M.P.; Fahrina, A.; Bilad, M.R. Hydrophilic Antimicrobial Polyethersulfone Membrane for Removal of Turbidity of Well-Water. *Water* **2022**, *14*, 3769. [[CrossRef](#)]
31. Saleem, H.; Goh, P.S.; Saud, A.; Khan, M.A.W.; Munira, N.; Ismail, A.F.; Zaidi, S.J. Graphene Quantum Dot-Added Thin-Film Composite Membrane with Advanced Nanofibrous Support for Forward Osmosis. *Nanomaterials* **2022**, *12*, 4154. [[CrossRef](#)]
32. Tian, H.; Wu, X.; Zhang, K. Tailoring Morphology and Properties of Tight Ultrafiltration Membranes by Two-Dimensional Molybdenum Disulfide for Performance Improvement. *Membranes* **2022**, *12*, 1071. [[CrossRef](#)] [[PubMed](#)]